

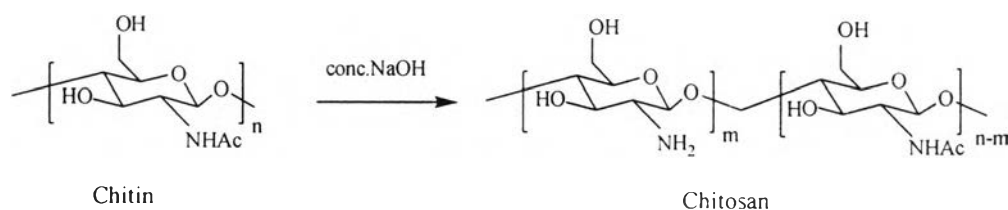


## CHAPTER II

### THEORY AND LITERATURE REVIEW

#### 2.1 Chitosan

Chitin, structurally similar to cellulose, is the natural polysaccharide which forms part of exoskeleton of crustaceans such as crabs and shrimps. Chitosan, a linear polycationic biopolymer, is prepared by alkaline *N*-deacetylation of chitin. Chemical structures of chitin and chitosan are shown in Scheme 2.1. Chitosan mainly consists of 2-amino-2-deoxy-D-glucose (GlcN) repeating unit with a small amount of 2-acetyl-2-deoxy-D-glucose residues. The amount of GlcN unit in chitosan is generally referred to the percent degree of deacetylation or % DD, influencing its physical, chemical properties as well as biological activities. Various techniques can be used for determination of % DD such as IR [1], NMR [2], and metachromatic titration [3].



**Scheme 2.1** Structures of chitin and chitosan.

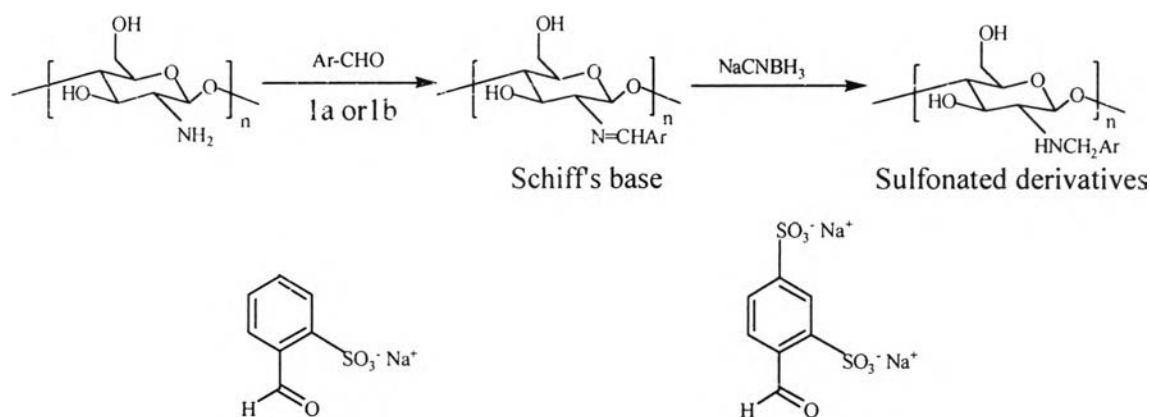
As a natural renewable resource, chitosan has a number of unique properties such as the physical, chemical, mechanical and biological properties including antimicrobial activity, nontoxicity, and biodegradability, which attract scientific interest in such fields as biotechnology, pharmaceuticals, cosmetics, agriculture, food science, and textiles. Due to its reactive amino and hydroxyl groups, chemical modification of chitosan to achieve its derivatives is used to expand its application.

## 2.2 Charged Derivatives of Chitosan

Generally, chitosan is soluble in aqueous medium in the presence of a small amount of acids such as acetic acid, lactic acid and so on. Chitosan can dissolve in aqueous acidic medium below pH 6, it precipitates above this pH due to lost its cationic nature. The application of chitosan was limited owing to the insolubility in neutral or high pH region. To improve the solubility property, chemical modification by the introduction of charged functional groups to native chitosan is required. Chitosan has both reactive amino and hydroxyl groups, which can be used to chemically alter its properties under mild reaction conditions. This research is interested in introducing two charged functional groups, sulfonate group and quaternary ammonium group which impart chitosan to dissolve in neutral and high pH mediums. The following related publications have been reported on chemical modification by grafting both two charged functionalities to the amino and/or hydroxyl groups.

In 1992, Muzzarelli prepared *N*-sulfofurfuryl chitosan and sulfoethyl *N*-carboxymethyl chitosan by reacting chitosan with the sodium salt of 5-formyl-2-furansulfonic acid and 2-chloroethanesulfonic acid, respectively. The <sup>13</sup>C NMR and FTIR spectra showed typical signals of furane carbon. Circular dichroism measurements were used to indicate its polyampholyte nature. The chelating reaction with metal ion was used to prove the chelating ability [4].

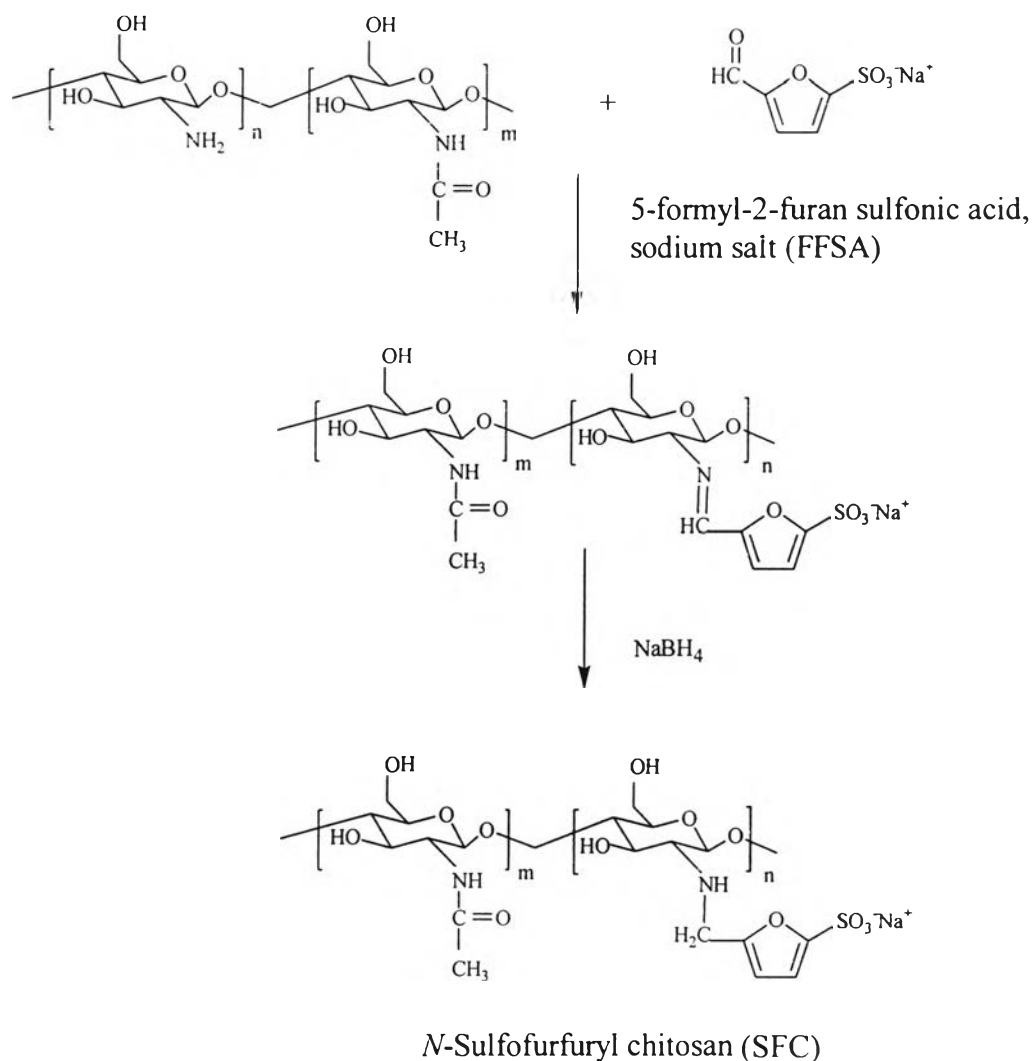
In 1997, Grégorio *et al.* synthesized *N*-benzyl sulfonated derivatives of chitosan by reactions with 2-formylbenzene sodium sulfonate and 4-formylbenzene sodium disulfonate in the presence of sodium cyanoborohydride. One-dimensional and two-dimensional NMR spectroscopies were used to characterize the structure of both products [5].



**Scheme 2.2** Synthesis of sulfonate derivatives of chitosan [5].

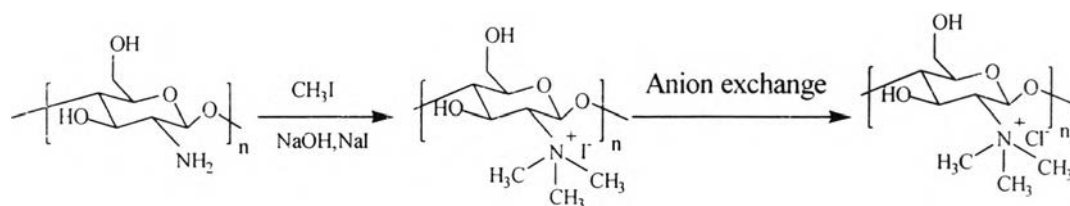
In 1998, Mansoor synthesized an amphoteric derivative of chitosan, *N*-sulfofurfuryl chitosan, by reductive alkylation using the sodium salt of 5-formyl-2-furansulfonic acid as a reagent. The synthesized sulfonated chitosan was found to be soluble in aqueous medium over a wide pH range. *In vitro* blood compatibility of the sulfonated chitosan was evaluated by measuring the number of adherent platelets and the extent of platelet activation. The sulfonated chitosan appeared to possess non-thrombogenic properties and may be suitable for some blood-contacting applications [6].

In 1999, Hitoshi, *et al.* prepared *N*-acylated chitosan derivatives via ring-opening reactions with various cyclic acid anhydrides and *N*-alkylation reactions with various aldehydes, monosaccharides and disaccharides in aqueous MeOH system.  $^1\text{H}$  and  $^{13}\text{C}$  NMR spectroscopies were used to characterize all products. The *N*-acyl and *N*-alkyl chitosan derivatives having carboxyl and sulfate group showed the solubility at basic pH region. Some of chitosan derivatives substituted with saccharides showed the solubility at all pH ranges [7].



**Scheme 2.3** Synthesis of *N*-sulfofurfuryl chitosan [6].

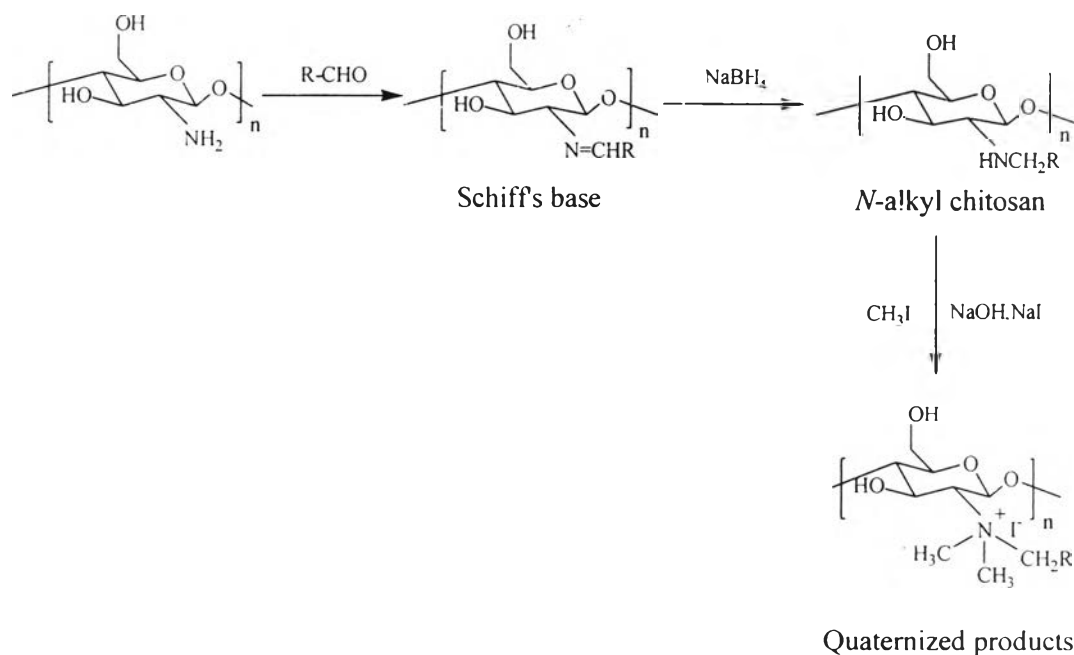
In 1986, Domard, *et al.* reported the conditions for preparation of the *N*-trimethyl chitosan or quaternary ammonium chitosan (QAC). The reaction was performed between chitosan and methyl iodide in the presence of sodium hydroxide (Scheme 2.4). The obtained product showed higher hydrophilicity than native chitosan in a broader pH range, especially at the physiological pH value (7.4) [8].



**Scheme 2.4** Synthesis of quaternary ammonium chitosan (QAC).

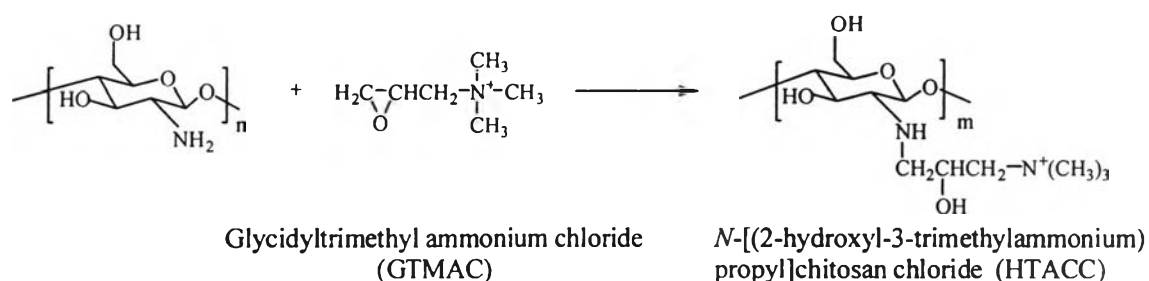
To increase the degree of substitution, Sieval, *et al* modified the reaction by adding methyl iodide in two and three steps, resulting in an increase of degrees of quaternization to 80% and >80% , respectively [9].

Kim, *et al.* were interested in antimicrobial activity of quaternary ammonium derivatives of *N*-alkylated chitosan. They synthesized *N*-alkyl chitosan by introducing alkyl groups into the amino groups of chitosan *via* Schiff's base intermediates. These compounds were then quaternized by reaction with methyl iodide (Scheme 2.5) [10].



**Scheme 2.5** Synthesis of quaternary ammonium salt of *N*-alkyl chitosan.

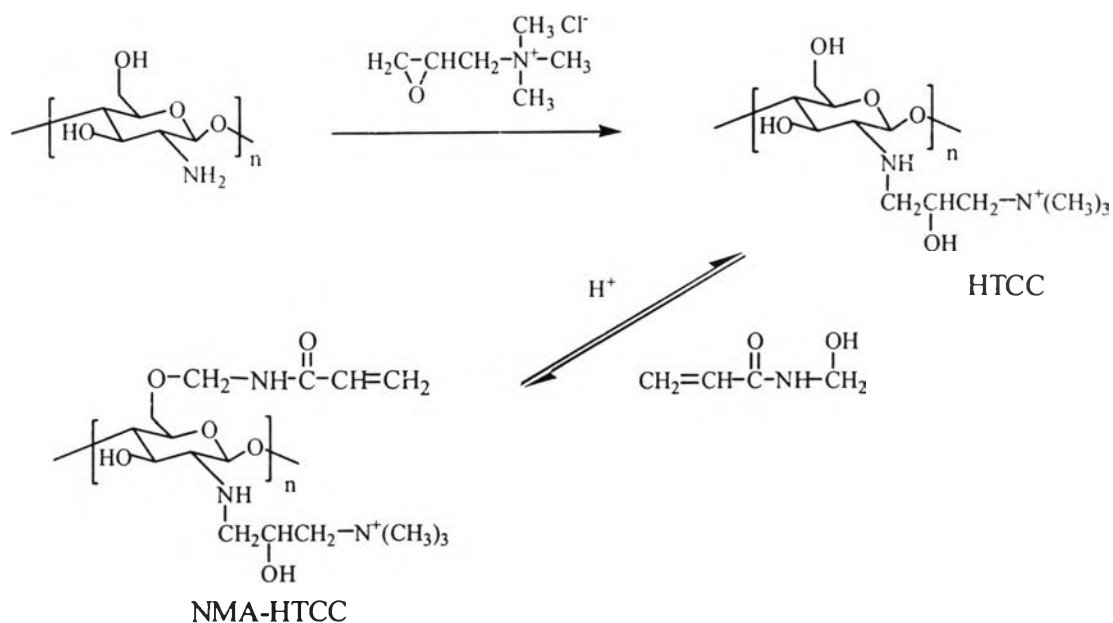
Other quaternized derivatives imparting antimicrobial activity to textile finishing were also suggested by Seong, *et al.* They synthesized a quaternary ammonium derivative of chitosan, *N*-(2-hydroxy)propyl-3-trimethyl ammonium chitosan chloride (HTACC), using a reaction of glycidyltrimethylammonium chloride (GTMAC) and chitosan (Scheme 2.6). HTACC showed superior antimicrobial activity to chitosan due to the quaternary ammonium group [11].



**Scheme 2.6** Synthesis of *N*-[(2-hydroxy-3-trimethylammonium)propyl]chitosan chloride (HTACC).

In 2003, Kim, *et al.* also synthesized HTACC and studied its antimicrobial activity against *Streptococcus mutans*, a principal etiological agent of dental caries in humans. The resulting HTACC exhibited the growth inhibition of above 80% against *S. mutans* after 5 h, whereas chitosan showed the growth inhibition of above 10% [12].

In 2004, Lim, *et al.* reported about a water-soluble chitosan derivative, *N*-[(2-hydroxy-3-trimethylammonium)propyl]chitosan chloride (HTCC), which was prepared by reacting chitosan with glycidyltrimethylammonium chloride (GTMAC). The HTCC was further modified by reacting with *N*-methylolacrylamide (NMA) to prepare a fiber-reactive chitosan derivative, *O*-acrylamidomethyl-HTCC (NMA-HTCC). The NMA-HTCC has an excellent antimicrobial activity against both *S. aureus* and *E. coli* as compared to chitosan, which does not dissolve in pH 7.2 and does not show any antimicrobial activity under this condition [13].



**Scheme 2.7** Synthesis of the HTCC and NMA-HTCC [13].

### 2.3 Polymer Adsorption

Adsorption of polyelectrolyte is governed by a complex interplay between molecular weight, solvent quality, interaction energy between the monomers and surface, the polyelectrolyte charge, the surface charge and the ionic strength. The usual description of conformations at an adsorbing interface is in terms of three types of subchains: trains, which have all their segments in contact with the substrate, loops, which have no contacts with the surface and connect two trains, and tails which are non adsorbed chain ends [14].

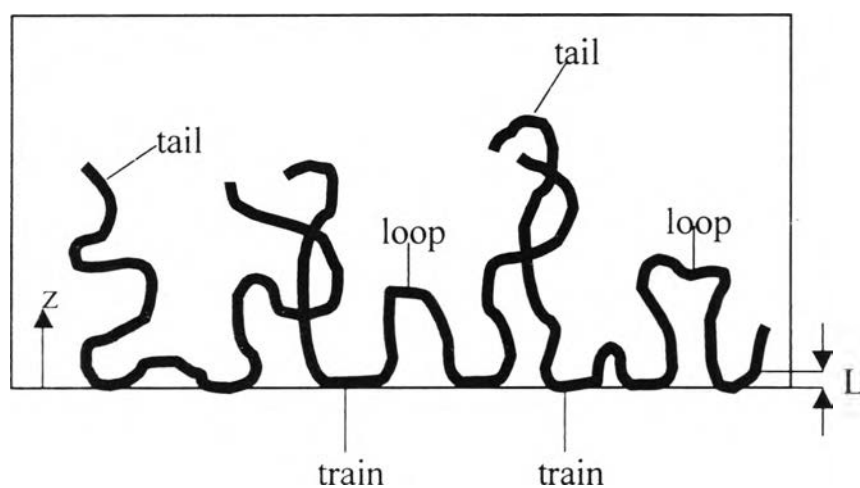


**Figure 2.1** Pictorial representation of an adsorbed polymer layer, indicating loops, tails and trains ( $L$  : thickness of chain) [14].

The amount of adsorbed weak polyelectrolyte depends strongly on charge density, controlled by ionic strength and pH. If the polyelectrolyte is fully charged, the adsorption layer is thin (chains with few loops and tails) and electrostatic repulsion opposes further adsorption. Increasing salt concentration reduces this repulsion, more polymer adsorbs and the layer becomes thicker and also more extended. The adsorption also increases with increasing molecular weight of the polymer. Polymer segments tend to form more loops, tails and eventually extended chains as the adsorbed amount and layer thickness increase. At very high ionic strength, however, where all charges on polymer segments are completely screened, a more random coil-like conformation with a smaller radius of gyration is more favorable than the extended chain.

#### **2.4 Layer-by-Layer Adsorption**

The fabrication of ultrathin polymer films on modified surfaces of material is important for various scientific and biological fields in order to modify the intact characteristics of these surfaces exposed to biological system. In most cases, the material characteristics seem to be governed by the chemical composition of the surface. Coating a substrate surface with polymeric ultrathin films can maintain the original mechanical properties and/or fine structure of the substrate.

The sequential adsorption of oppositely charged polyelectrolytes (PE) by layer-by-layer (LBL) deposition technique is an efficient method for obtaining multilayer thin films with well-defined thickness, composition and functionalities. Due to the simplicity and the versatility of the buildup process, this technique opens enormously new opportunities to achieve the ideal model surface for use in applications such as biosensing [15], separation membrane [16] and optical devices [17]. LBL process was first introduced by Decher *et al.* in 1991. They have demonstrated the basic principle of buildup of multilayer materials using alternating adsorption of PE [18].



The crucial feature of the sequential adsorption is the excessive adsorption at every stage of the polycation/polyanion assembly, which led to the recharging of the outermost surface at every step of film formation (Figure 2.2). Hence, the electrostatic interaction between the surface and polyions in solution is usually considered as the driving force for multilayer formation. The adsorption behavior of polyelectrolytes is influenced by a number of factors such as the charge density [19], the ionic strength or the pH of the solutions and the solvent quality [20].

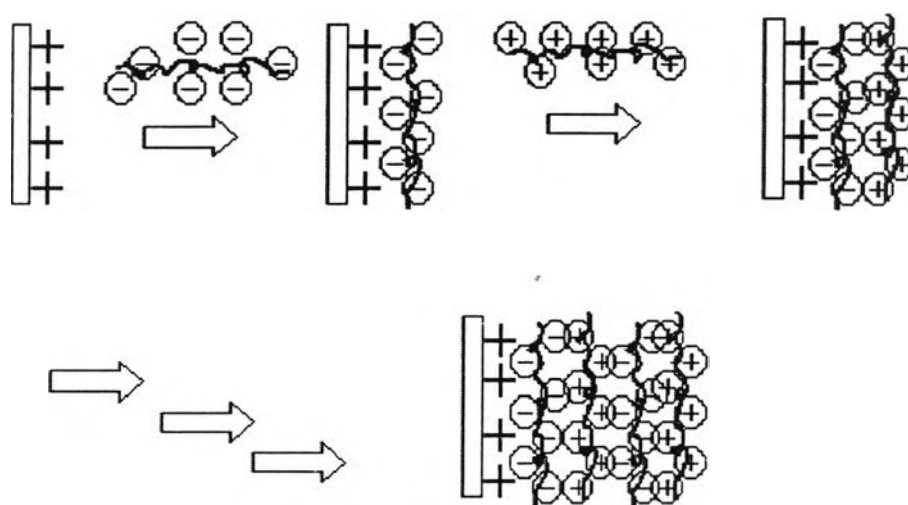


**Figure 2.2** Alternate layer-by-layer adsorption of polyanion and polycation onto a positively charged substrate.

Recently, many research publications reported the use of the layer-by-layer adsorption to prepare ultrathin polymer film for biomedical applications.

In 1994, Yuri, *et al.* prepared densely packed charged virus sandwiched in multilayer films of charged polyelectrolytes by successive adsorption of poly(styrene sulfonate) (PSS) and poly(allylamine hydrochloride) (PAH). It was demonstrated that the surface created by particle deposition was smooth. Very precise data on the thicknesses of sublayers were derived from suitable model fitting [21].

In 1997, Chen, *et al.* sequentially adsorbed PAH and PSS on three organic polymer substrates: PET, PET-CO<sub>2</sub><sup>-</sup> and PET-NH<sub>3</sub><sup>+</sup>. The wettability of multilayer films is largely controlled by the identity of the outermost polyelectrolyte layer. The thickness of the individual layers which XPS and contact angle data indicating their extremely thin (2-6 Å) is affected by the substrate surface chemistry and can be controlled by the ionic strength. The deposition stoichiometry is also affected by substrate chemistry and solution ionic strength. Peel tests indicated that the multilayer assemblies had significant mechanical strength [23].

In 2000, Guy, *et al.* investigated the interaction between poly(styrene sulfonate) (PSS) and polyallylamine (PAH) multilayers with human serum albumin (HSA). The results showed that the underlying complexity of concentration and pH dependent adsorption/desorption equilibrium often simply termed “protein adsorption” was the result of antagonist competing interactions that were mainly of electrostatic origin [24].

In 2005, Köstler, *et al.* fabricated poly(diallyldimethylammonium chloride (PDADMAC)/PSS multilayer films on pretreated polymeric (PET and PTFE) and inorganic (glass slide and silicon wafer) substrates. Contact angle measurements showed a regular odd-even pattern even for the first PDADMAC/PSS layers on sufficiently smooth and hydrophilic substrates. The surface thermodynamic data indicated an increase in coating density with increasing layer number. The effect of thicker layers and a more coiled conformation by deposition from salt-containing solution were also noted by surface thermodynamic component [25]. In the same year, Kolasinśka, *et al.* prepared multilayer films of PAH/PSS by using layer-by-layer deposition technique on various support materials. Periodic oscillations in contact angle values were observed for multilayer terminated by PAH and PSS, respectively and the variations in contact angle values strongly depended on the adsorption conditions and multilayer treatment after deposition. The optimum ionic strength of polyelectrolyte solution was used for deposition on wetting of multilayer films. PEI was modified as a first layer of PAH/PSS multilayer film to investigate the influence of the first layer [26].

In view of alternate layer-by-layer assembly of cationic chitosan with oppositely charged polyelectrolytes, the following related publications have been reported.

In 1998, Yuri, *et al.* prepared biocompatible molecular surfaces by an alternate assembly of cationic chitosan and anionic PSS at pH 4. Film growth and its dependence on ionic strength were analyzed by the QCM method. In addition, surface structure of the ultrathin films was examined by non-contact atomic force microscopy [27].

In 2000, Takeshi, *et al.* studied the alternating anti-vs procoagulation activity of ultrathin polymer films prepared by layer-by-layer assembly technique against human blood. Dextran sulfate (Dex) and chitosan were selected as polymers with anti-and pro-coagulation activities, respectively. The layer-by-layer assembly of these polymers was quantitatively analyzed by a quartz crystal microbalance (QCM). They also investigated the influence of salt concentration in the polymer aqueous solutions on the assembly process, which ultimately led to thicker films. This study demonstrated that biocompatibility of multilayers can be controlled. [28] Later in 2002. Takeshi, *et al.* continued their study on multilayer systems. They varied concentration of NaCl as 0.2, 0.5 and 1 M. They found that the apparent film thickness increased upon increasing NaCl concentration. There was a critical concentration for the alternating activity; above a concentration of 0.5 M NaCl, both anti-and procoagulation could be observed on the dextran sulfate and chitosan surfaces, respectively. They also studied the formation of assembled film from a combination of chitosan and heparin, but the activity was different from that of the former system. They suggested that the polymer species and/or the assembly conditions are key factors for realizing the alternating bioactivities of films prepared by the layer-by-layer assembly [29].

In 2004, Feng, *et al.* fabricated the polyelectrolyte complex multilayer of hyaluronic acid (HA)/chitosan with two strategies and characterized by atomic force microscopy (AFM). The films exhibited cluster features on the substrate with the

first strategy. The films also exhibited a more homogenous feature, a nice miscibility at nanometer scale and had a lower roughness than pure chitosan films [30].

In 2005, Fu, *et al.* constructed a kind of heparin (anti-adhesive agent) and chitosan (antibacterial agent) multilayer film onto aminolyzed PET films. The contact angle and UV results verified the progressive buildup the multilayer film by alternate deposition of the electrolyte. The properties of films were investigated by contact angle, atomic force microscopy (AFM), lateral force microscopy (LFM) and UV spectroscopy. The multilayer films not only reduced the bacterial adhesion but also kill the bacterial adhered onto the surface. The assembly pH represented the important influence on both surface properties of the films, i.e., the composition, roughness, wettability and their anti-adhesive and antibacterial properties [31].

## 2.5 Protein Adsorption on Chitosan Surface

Protein adsorption is a very complex process and has for the most part resisted efforts to predict it quantitatively. The interaction of proteins with solid surfaces is a fundamental phenomenon with significance for nanotechnology, biomaterials and biotechnological processes. In the biomaterials field, protein adsorption is the first step in the integration of an implanted device or material with tissue. This protein adsorption in turn results in platelet adhesion and activation on the surface of the material, thrombus formation, and ultimately device failure. The interaction forces between protein molecules and surface can be classified as follows: (1) Van der Waals, (2) hydrophobic interactions, (3) hydrogen bonding, and (4) ionic interactions.

In 1994, Yuri, *et al.* prepared multilayer films by means of alternate adsorption of positively charged globular protein (myoglobin or lysozyme) and anionic poly 4-(styrene sulfonate). Regular growth alternate adsorption cycles were analyzed by UV spectroscopy and quartz crystal microbalance (QCM) [22].

Surface modification using hydrophobic polymers has also been shown to affect protein adsorption. The surface of chitosan films was modified using acid

chloride and acid anhydride. The improved surface hydrophobicity by the stearyl groups promoted protein adsorption. In addition, selective adsorption behavior was observed in the case of the chitosan films modified with anhydride derivatives. Lysozyme adsorption was enhanced by H-bonding and charge attraction with the negative charge dissociated from the anhydride grafted surface. While the amount of albumin adsorbed was decreased possibly due to the repulsion between the modified surface and albumin [32].

In 2002, Johan and Petti prepared thin chitosan films by glutaraldehyde crosslinking of chitosan onto APTES coated surfaces. Biocompatibility of the supported thin film was analyzed after incubating in serum or plasma. Polyclonal antibodies towards a few selected serum proteins were used to detect the binding and activation of complement factors and the intrinsic pathway of coagulation proteins. The adsorbed amounts of serum and antibodies were quantified by single wavelength null ellipsometry. However, acetylation turned the chitosan coating into a strong alternative pathway activator. Large amounts of fibrinogen and other plasma proteins bound to chitosan but not to acetylated chitosan. The present results confirm that chitosan can activate the complement cascade and that the activation depends on degree of acetylation [33].

## **2.6 Surface Characterization**

### **2.6.1 Quartz Crystal Microbalance (QCM)**

The QCM is based on the principle of impedance analysis, which enables the determination of frequency changes (mass) and changes in the dissipation coefficient (viscoelastic properties) of adsorbed or deposited layers on a quartz crystal. If a mass is adsorbed or placed onto the quartz crystal surface, the frequency of oscillation changes in proportion to the amount of mass.

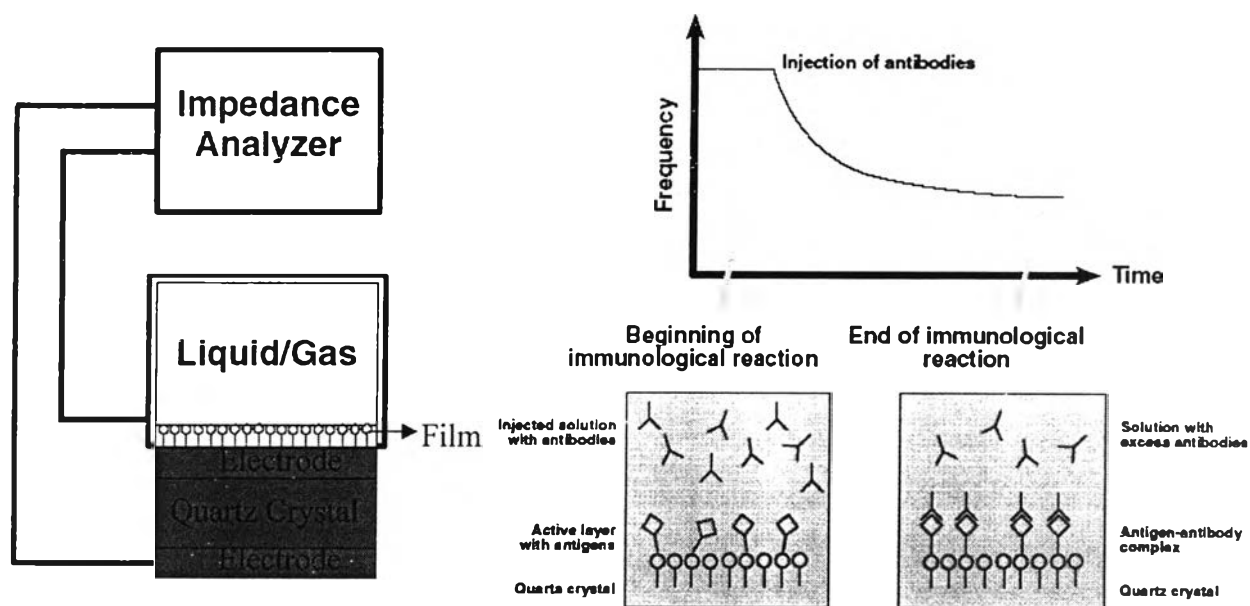


**Figure 2.3** Diagram of quartz crystal microbalance (QCM).

If a rigid layer is evenly deposited on one or both of the electrodes the resonant frequency will decrease proportionally to the mass of the adsorbed layer according to the Sauerbrey equation:

$$\Delta f = -[2 \times f_0^2 \times \Delta m] / [A \times (\rho_q \mu_q)^{1/2}] \quad (1)$$

$\Delta f$  : measured frequency shift,

$f_0$  : resonant frequency of the fundamental mode of the crystal,

$\Delta m$  : mass change per unit area,

$A$  : piezo-electrically active area,

$\rho_q$  : density of quartz, 2.648 g/cm<sup>3</sup>,

$\mu_q$  : shear modulus of quartz, 2.947 x 10<sup>11</sup> g/cm x s<sup>2</sup>

## 2.6.2 Contact Angle Measurement

One of the most sensitive methods known for obtaining surface tension information of solids is contact angle. This method is unique in that the equipment required is relatively simple and inexpensive. The basis of the measurement of solid surface tension by contact angle is the equilibrium of the three-phase boundary, shown in Figure 2.3 which can be described by Young's equation. If the angle  $\theta$  is less than  $90^\circ$  the liquid is said to wet the solid. If it is greater than  $90^\circ$ , it is said to be non-wetting. A zero contact angle represents complete wetting.

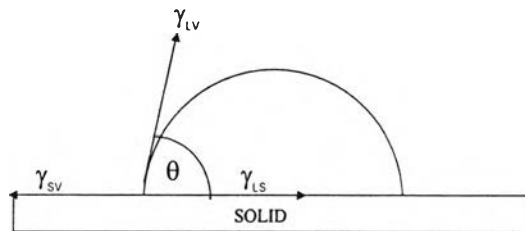


**Figure 2.4** Equilibrium of the three-phase boundary on solid surface.

$$\text{Young's Equation : } \gamma_{sv} - \gamma_{ls} = \gamma_{lv} \cos\theta \quad (2)$$

$\gamma_{LV}$ : interfacial tension between liquid and vapor phases

$\gamma_{SV}$ : interfacial tension between solid and vapor phases

$\gamma_{LS}$ : interfacial tension between liquid and solid phases

In this research, air-water contact angle was used for determining the wettability and the stratification of multilayer films.

### 2.6.3 Attenuated Total Reflectance Infrared Spectroscopy (ATR-IR)

The infrared beam from the spectrometer is focused onto the beveled edge of an internal reflection element (IRE). The beam is then reflected, generally numerous times, through the IRE crystal, and directed to a detector (Figure 2.5).

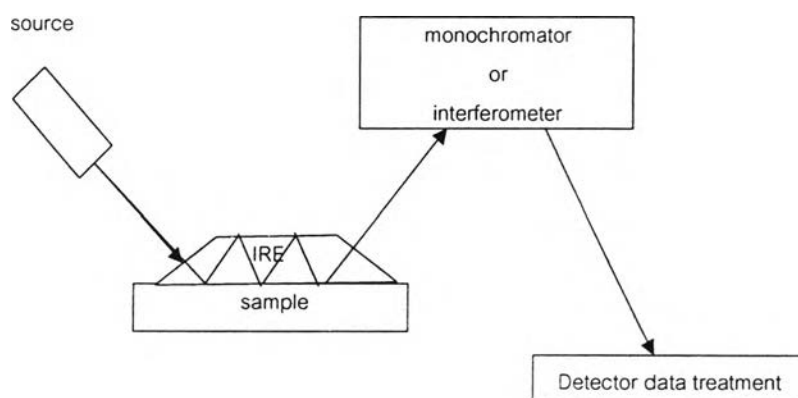


**Figure 2.5** Diagram of ATR-IR.

The radiation can penetrate a short distance into the sample, thus interacts with any functionalities existing within that depth. The depth of penetration ( $d_p$ , defined as the distance from the IRE-sample interface where the intensity of the evanescent wave decays to  $1/e$  of its original value) can be calculated using the formula in the following equation:

$$d_p = \frac{\lambda}{2\pi n_p (\sin^2 \theta - n_{sp}^2)^{1/2}} \quad (3)$$

where  $\lambda$  = wavelength of the radiation in the IRE,  $\theta$  = angle of incidence,  $n_{sp}$  = ratio of the refractive indices of the sample vs. IRE, and  $n_p$  = refractive index of the IRE.



In this study, ATR-IR was used for identifying functional groups on the surface of the films. Sampling depth of characterization is 1-1.5  $\mu\text{m}$ .

